9950-677

DRL No. 135
Technical Report: MRI - 289

DOE/JPL - 955676-1
Distribution Category UC - 63

ANALYSIS OF DEFECT STRUCTURE IN SILICON

Silicon Sheet Growth Development for the Large Area Silicon Sheet Task of the Low-Cost Solar Array Project.

FINAL REPORT

by
R. Natesh
M. Mena
M. Plichta
J. M. Smith
M. A. Sellani

April, 1982

JPL Contract No. 955676

The JPL Low-Cost Silicon Solar Array Project is sponsored by the U.S. Department of Energy and forms part of the Solar Photovoltaic Conversion Program to initiate a major effort toward the development of low-cost solar arrays. This work was performed for the Jet Propulsion Laboratory, California Institute of Technology, by agreement between NASA and DOE.

MRI Materials Research, Inc.

Research
Development
Consulting and Testing
Of Materials

700 South 790 East
Centerville, Utah 84014
Telephone: (801) 298-4000

DRL No. 135
Technical Report: MRI - 289

DOE/JPL - 955676-1
Distribution Category UC - 63

ANALYSIS OF DEFECT STRUCTURE IN SILICON

Silicon Sheet Growth Development for the Large Area Silicon Sheet Task of the Low-Cost Solar Array Project.

FINAL REPORT

by
R. Natesh
M. Mena
M. Plichta
J. M. Smith
M. A. Sellani

April, 1982

JPL Contract No. 955676

The JPL Low-Cost Silicon Solar Array Project is sponsored by the U.S. Department of Energy and forms part of the Solar Photovoltaic Conversion Program to initiate a major effort toward the development of low-cost solar arrays. This work was performed for the Jet Propulsion Laboratory, California Institute of Technology, by agreement between NASA and DOE.

MRI Materials Research, Inc.

Research
Development
Consulting and Testing
Of Materials

700 South 790 East
Centerville, Utah 84014
Telephone: (801) 298-4000

TECHNICAL CONTENT STATEMENT

CONTENTS

LIST OF FIGURES

LIST OF TABLES

SECTION I

SUMMARY

The analyses of one hundred and ninety-three (193) silicon sheet samples, approximately 880 square centimeters, for twin boundary density, dislocation pit density, precipitate density, and grain boundary length has been accomplished in the past contract period. One hundred and fifteen (115) of these samples were manufactured by Crystal Systems, Inc., using their Heat Exchanger Method (HEM), thirty-eight (38) by Mobil Tyco using Edge-defined Film-fed Growth (EFG), twenty-three (23) by Honeywell using the Silicon-on-Ceramics (SOC) process, and ten (10) by Westinghouse using the Dendritic Web process. Seven (7) solar cells were also step-etched to determine the internal defect distribution on these samples.

Procedures have been developed for the quantitative characterization of structural defects such as dislocation pits, precipitates, twin & grain boundaries using a QTM 720 Quantitative Image Analyzing System interfaced with a PDP 11/03 mini-computer. These procedures were routinely applied to all the samples. Characterization of the grain boundary length per unit area for polycrystalline samples was done by using the "intercept method" on an Olympus HBM Microscope.

This report describes the steps involved in the characterization of

structural defects in the various types of solar cell materials analyzed. A summary of results as well as discussions of the data are also presented.

SECTION II

INTRODUCTION

The main objective of this program was to develop imaging techniques to subsequently allow rapid, reproducible, and accurate evaluation of silicon sheet defect structure. Secondly, defect data accumulated for many samples would allow for potential cross correlation between structures revealed and specific sheet fabrication technique and/or efficiency. Structural defects that were quantified included grain and twin boundaries, precipitates, and dislocations. Quantitative characterization of these structural defects,. which have been revealed by etching the surface of silicon samples, can then be performed using a Quantimet 720 Image Analyzer.

The silicon sheet samples were originally obtained by JPL from different manufacturers. Each of these manufacturers use their own crystal growth and fabrication techniques and, therefore, the various types of silicon produced contain a variety of trace impurity elements and structural defects. The most important criteria in evaluating the various silicon types for terrestrial solar cell applications are: (i) cost and (ii) conversion efficiency. At present, the solar cells with highest conversion efficiency are made of high purity silicon single crystals, which are free from structural defects such as dislocations, twin boundaries, precipitate particles, etc. But these crystals and subsequent processing are very expensive and may not meet DOE technology requirements. On the other hand, silicon crystals such as Edge-defined Film-fed Growth (EFG) ribbons, Silicon-on-Ceramic (SOC), Wacker, etc, are NOT single crystals; but made of highly ordered crystals which contain large and differing numbers of dislocations, twin boundaries, grain boundaries, and precipitates compared to the premium grade or Czochralski grown silicon.

The following important questions must be answered to evaluate low and high cost silicon sheets: (i) What effect do these defects have on conversion efficiency? (ii) Of the various types of defects, which defect/defects severely affects conversion effects conversion efficiency? (iii) At what concentrations does this effect become significant? (iv) Is there a rapid, accurate, quantitative method that can be used routinely as a Quality Assurance tool?

Quantitative analysis of surface defects was developed and is being performed by using a Quantimet 720 Quantitative Image Analyzer. This system can differentiate and count 64 shades of grey levels between black and white contrasts. In addition, it can characterize structural defects by measuring their length, perimeter, area, density, spatial distribution, frequency distribution (in any preselected direction), and is programmable in these measurements. However, the Quantitative

Image Analyzer is extremely sensitive to optical contrasts of various defects. Therefore, to obtain reproducible results, the contrasts produced by various defects must be similar and uniform for each defect types along the entire surface area of samples to be analyzed. To achieve this, a chemical cleaning and polishing technique has now been perfected for silicon samples from Mobil Tyco, Wacker, Motorola, and IBM. The cleaning and polishing preparation technique produces a very clean and even surface for silicon crystals suitable for analyses by the QTM 720 Image Analyzer. We have now obtained quantitative information from a variety of silicon crystals.

SECTION III

TECHNICAL DISCUSSION

A. Chemical Polishing:

The detailed procedures of crystal cleaning, chemical polishing, and chemical etching have been thoroughly discussed in previous reports[1,2] and only a summary of these procedures shall be presented in this report.

The silicon samples received may be divided into two groups: those that need mechanical polishing prior to chemical polishing, and those that can be chemically polished directly. Silicon samples cut from ingots such as the HEM samples belong to the first group while samples grown using ribbon technology such as the EFG and the Dendritic Web belong to the second group.

The mechanical polishing consisted of hand lapping the samples using a 600 grit polishing paper followed by wheel lapping on a Jarrett Automatic Polishing machine using diamond paste abrasives of 30, 7, and 1 micron sizes. Each of the polishing steps took approximately ten (10) minutes. Thus, forty (40) minutes was the mechanical polishing time for each sample.

The silicon samples are then swabbed with trichloroethylene (TCE) to remove any organic substances on the sample surfaces. The remaining residues and water spots are removed by an acetone rinse followed by an ethyl alcohol rinse. The silicon surfaces are then dried by blowing freon gas over them.

An acid-resistant coating is then applied to one surface of the silicon sample in order to prevent this surface from being attacked by the polishing and etching solutions. This allows JPL to fabricate the unpolished surface of the silicon samples into solar cells and measure their conversion efficiencies. MRI is also able to complete etching and defect analyses on the unprotected surfaces and correlate the type and density of structural defects obtained to the conversion efficiencies that JPL measured.

Of the various coating materials studied, Apiezon Wax showed the greatest resistance to the polishing and etching solutions. Small amounts of Apiezon Wax are dissolved in TCE and applied by a fine paint brush to one of the silicon sample surfaces. Apiezon wax is also used in preserving the JPL orientation mark. The coated surface is then baked for 10 minutes at 125°C $\pm$ 10°C. This evaporates the TCE and allows the wax to flow uniformly on the surface.

The sample is then allowed to cool for about 3 to 5 minutes and then immersed in concentrated hydrofluoric acid at room temperature for 3 minutes. This removes any silicon oxide on the sample surface. The sample is rinsed in deionized water and washed in ethyl alcohol. Freon gas is again used to dry the sample surface. All the steps discussed above are necessary prior to chemical polishing.

The polishing solution being used is a 1:2:3 ratio by volume mixture of concentrated nitric, hydrofluoric, and acetic acids respectively. All acids used are of Electronic Grade, Low Sodium MOS quality. The polishing solution is heated to 50 °C ± 3 °C in a teflon beaker on a hot plate. The silicon sample is then immersed in this solution. Polishing times differ between sample types, and a test run is always performed on a new batch of samples received to determine the optimum polishing time. For the work included in this report, polishing times varied from 5 seconds for some Mobil - Tyco EFG samples to 90 seconds for some HEM samples. Also, the polishing solution was diluted to 1:2:7 ratio for the SOC samples. No chemical polishing was required for the Dendritic Web samples.

Polishing is done in increments of 15 - 20 seconds for samples that require extensive chemical polishing and the extent of polish is determined after each step by viewing the samples under an optical microscope. The sample is immediately immersed in deionized distilled water, after it is removed from the polishing solution, to stop the polishing reaction. After five minutes, the sample is rinsed in ethyl alcohol and dried with freon gas. The sample is now ready for chemical etching.

B. Chemical Etching:

Several etching solutions have been tested in previous work and the one that was found suitable for revealing structural defects on several types of silicon sheet materials is a variation of the Sirtl etching solution. This variation, labeled Etching Solution III by MRI, consistsof 10 grams of CrO_3 in 60 ml. of deionized distilled water and an equal volume of concentrated hydrofluoric acid.

The etching treatment by Etching Solution III resulted in an optical resolution of 10^{-4} cm. for twin boundaries and an optical density resolution of 10^7 dislocations per cm^2. at magnification of 800X and above. A higher resolution, however, can be achieved by using higher magnifications.

An average of 45 to 50 seconds of etching in Etching Solution III at room temperature has been found to distinctly reveal grain boundaries, twin boundaries, and dislocations. Etching Solution III was used on all the 193 silicon sheet material analyzed with some modifications and was found to produce high quality defect structures with a minimum of overlapping and contrast variations between each type of defect.

C. QTM 720 Measurement of Dislocation Pits, Twin Boundaries and Precipitate Particles:

A quantitative Image Analyzer (Quantimet 720: Cambridge - Imanco, Monsey, N. Y.) linked to a Digital Equipment Corporation PDP 11/03 computer is being used for the quantitative analysis of dislocation pit density, twin density, and precipitate particle density in etched silicon samples. The flow chart for the QTM Operation and Data Reduction used in the latest version of the computer program for defect analysis is given in Figure 1. The following data are collected and compiled by the system: number of features and areal density, mean free path between features (measured in horizontal and vertical directions), and length of feature per unit area of the sample.

Before any measurements are made, the optical and electronic systems of the QTM 720 are adjusted to provide for optimum detection of the structural defect being analyzed. Then the PDP 11/03 computer is prepared for operation. Detailed discussions of these procedures have been given in previous reports.[2,3]

Measurements are then made for the average defect/feature area. This feature could be a dislocation pit, twin boundary, precipitate particle, etc. Five or six fields in each sample are chosen and observed at the desired magnification, which is usually 800X. The average feature area is obtained by dividing the total feature area as detected by the QTM 720 by the total number of features in these five of six fields. Fields with a minimum overlap of features are chosen in the determination of the average feature area. The average feature area is one of the required inputs into the "Defects in Silicon" computer program. This procedure allows for the calculation of the feature density even in fields where extensive feature overlap occurs.

After the average feature area is obtained and fed into the computer, the number of fields to be observed and the mode of scan are determined. MRI always takes the maximum number of fields that the sample surface and time limitations would allow.

Two modes of scanning are currently being used. For samples wherein a symmetrical distribution of defects is present, as in the Mobil Tyco samples, a single horizontal scan along the middle of the sample perpendicular to the growth direction is taken. Previous works [2,4] have shown that this procedure yields statistically sound results. For samples wherein the defects are distributed randomly on the sample surface, a square raster is used. The QTM 720 is equipped with an automatic stage control, and step sizes in the x-and y-directions can be pre-set. The step sizes are chosen so as to obtain the desired number of fields and cover the entire surface of the sample. The square raster mode of scanning is used on the HEM, SOC, and HAMCO samples. The size of the test field is chosen next. An attempt is always made to use the largest frame area of 500,000 picture point, but the non-flatness of the sample surface may dictate the use of a smaller area if focusing on the entire 500,000 picture point field becomes a problem. The quantitative characterization of the defects may now be initiated.

Given in Appendix I are samples of the computer teletype printouts generated by the procedures discussed above. Only a few are given in this report because of the large volume of computer printouts that were generated by all the samples, but these printouts are available in the individual Technical Reports [6-12].

The first paragraph in the printout gives the name of the program being used, the identification of the sample, and the type of defect being analyzed. The second paragraph lists: (1) the identification of the operator, (2) magnification being used, (3) units being used, (4) calibrated equivalent value of one picture point in the units being used, (5) the frame area, (6) the factor by which the QTM output is divided by to avoid overflow problems, and (7) the average feature area determined manually in the units of picture points.

The third paragraph lists the titles for the different measurements, which are explained below:

Field: indicates the sequence number of the field in which measurements were made.

No: denotes the total number of features detected in any given field. This number is obtained by dividing the total area of detected feature by the average feature area.

No./Area: denotes the computed number of features per um^2 or features per mm^2 in each field depending on the units being used.

<u>MFPV:</u> denotes the mean free path in the vertical direction. This quantity is the frame area divided by the vertical projection of all detected features in the field.

<u>MFPH:</u> denotes the mean free path in the horizontal direction. This is the horizontal analogue of MFPV.

<u>L/A:</u> denotes the length of detected feature per unit area. Disregard for dislocations.

D. Grain Boundary Length Measurement:

The grain boundary lengths per unit area of polycrystalline samples are measured using the intercept method which has been discussed previously.[5,7] This method consists basically of determining the number of times a grain boundary is intersected by a test line. From this, P_L, which is the number of intersections per unit length of the test line is obtained. The grain boundary length per unit area, L_A, is then calculated using the appropriate formula in Table 1. These measurements are all done using an Olympus HBM Microscope equipped with a video display. Table 2 gives a calibration of the video test grid for all the magnifications available on the microscope .

SECTION IV

RESULTS

A total of one hundred and ninety-three (193) samples have been quantitatively characterized in the past contract period. These samples were received from five different manufacturers and are distributed as follows:

1. Heat Exchanger Method	115
2. Edge-defined Film-fed Growth	38
3. Silicon-on-Ceramic	23
4 Dendritic Web	10
5. Solar Cells	7
a) EFG - 4	
b) HAMCO - 3	
Total	193

These samples were analyzed for twin boundaries, grain boundaries, dislocation pit, and precipitates. Twin boundary, dislocation pit, and precipitate density measurements were done using the QTM 720, while grain boundary length measurements were done using an Olympus HBM microscope. Data from these measurements are herein presented.

A. HEM Silicon Samples:

The HEM samples were received after they have been wafered and cut into approximately 2 cm x 2 cm coupons. The samples have not undergone any type of polishing and the surfaces were dull. Saw marks were also visible on the sample surfaces. Test samples were chemically polished to determine whether surfaces suitable for QTM 720 analysis can be produced. The results showed that mechanical polishing prior to chemical polishing was necessary for QTM analysis. The mechanical polishing procedures have been discussed in the previous section. Chemical polishing times ranged from 60 to 90 seconds, and etching time was 50 seconds.

The one hundred and fifteen HEM samples were received in two batches. The first batch[9] consisted of 24 single crystal and 19 polycrystalline samples cut from Wafer Numbers 4T-20, 4B-20, 3T-20, 3B-20, 103, 5 and 53. These samples were characterized for silicon carbide precipitate density, twin density, and grain boundary length. A few dislocation pits were also observed but were not quantitatively characterized. The dislocation pit density for these samples would be in the order of 10^2 pits per cm^2. This value was arrived at by comparison of these samples with other HEM samples in which the dislocation pit density was measured. For the single crystals, only silicon carbide precipitates were observed and measured. The results are given in

Table 3 This table shows that precipitate density ranges from 1.159 E-03 precipitates per μm^2 for sample A-17 to 1.503 E-02 precipitates per μm^2 for sample A-25. The average precipitate density of the single crystal samples is 5.149 E-03 precipitates per μm^2, (5×10^5 precipitates per cm^2) with a standard deviation of 3.347 E-03.

On the other hand, the polycrystalline samples were characterized for twin and grain boundaries, in addition to the silicon carbide precipitates, and the results are shown in Table 4. For the precipitate density, the values ranged from 1.697 E-03 precipitates per μm^2 to 1.207 E-02 precipitates per μm^2 for samples B-8 and B-1, respectively. The average precipitate density of the polycrystalline group is 4.384 E-03 precipitates per μm^2, (4×10^5 precipitates per cm^2) with a standard deviation of 3.490 E-03. Comparing the average precipitate densities of the single crystal and polycrystalline groups, there seems to be no significant difference between the values obtained. This suggests that no preferential precipitation of silicon carbide occurs on the polycrystalline samples. It was also observed that samples B-1, B-2, B-3 and A-25 which had the highest precipitate densities (10^6 precipitates per cm^2) were cut from the same wafer. (Wafer No. 53). This must have been influenced by the position of this particular wafer in the ingot. For the twin density, sample B-10 has the highest with 0.174 lines per cm^2 while sample B-9 has the lowest with no twin boundaries. There must have been some mistake in the inclusion of sample B-9 in the polycrystalline group because it also showed no grain boundaries. The average twin density of the "B" samples is 0.051.

For the grain boundary length per unit area, sample B-10 has the highest unit 0.838 mm per mm^2 while sample B-9 showed no grain boundaries. The average grain boundary length per unit area is 0.312 mm per mm^2 with a standard deviation of 0.222.

The second batch[11] of HEM samples consisted of seventy-two specimens which were cut from 14 wafers of Run 41-48C. A summary of the results of the measurements is shown in Table 5. The dislocation pit density ranges from 0.349 to 25.556 pits per mm^2, with an average of 3.752 pits per mm^2 which is equivalent to 375 pits per cm^2. The dislocation pit density was obtained manually because the dislocation pits and precipitate particles were of the same shade of contrast and size that the QTM 720 would not be able to distinguish one from the other. Therefore, the dislocation pit density was measured using an Olympus HBM microscope with a total magnification of 1100X.

The twin boundary density ranges from 0 to 124.943 lines per mm^2 with an average of 16.437 lines per mm^2. Finally, the grain boundary length ranges from 0 to 0.937 mm per mm^2, with an average of 0.315 mm per mm^2.

An average of all the data obtained for each of the wafers was also calculated and the results are shown in Table 6. This information will be useful in plotting defect concentrations as a function of position in the ingot. The distribution of silicon carbides and its concentration relative to the dislocation pits are shown in Figures 2 and 3.

B. EFG Silicon Samples:

The thirty-eight (38) EFG samples were received in two batches. The first batch[8] consisted of 25 samples and the second batch[12] consisted of 13 samples. The as-received surfaces of the EFG samples were shiny and relatively flat so that 5 seconds of chemical polishing was enough. A 45-second etch in Etching Solution III revealed the structural defects on the sample surface. These samples were characterized for dislocations, twin boundaries, and grain boundaries.

Table 7 shows a summary of the results for the twenty-five (25) samples in the first batch which consisted of Runs 17-139, CO_2 OFF; 17-139, CO_2 ON; 17-143, CO_2 OFF; 17-143 CO_2 ON; and 17-143. The dislocation pit density varies from 4.632 E-03 pits per um^2 (4.6×10^5 pits per cm^2) to 3.503 E-02 pits per um^2 (3.5×10^6 pits per cm^2). The twin density varies from 96.8 to 1192.7 lines per mm^2 and the grain boundary length per unit area varies from 0.112 to 1.326 mm per mm^2. The run averages were also calculated and the results are shown in Table 8.

Run 17-139, CO_2 OFF has the lowest average dislocation pit density with 1.299 E-02 pits per μm^2 (1.3×10^6 pits per cm^2) while run 17-146 has the highest average dislocation pit density at 2.599 E-02 pits per μm^2 (2.6×10^6 pits per cm^2). Run 17-139, CO_2 ON has the lowest average twin density with 212.8 lines per mm^2 while run 17-139, CO_2 OFF has the highest average twin density with 584.9 lines per mm^2. With respect to the average grain boundary length, run 17-139, CO_2 OFF has the lowest with 0.271 mm per mm^2 while run 17-139, CO_2 ON has the highest at 0.568 mm per mm^2.

From the averages calculated in Table 8, the use of a CO_2 atmosphere does not seem to have any effect on the density of structural defects. For run 17-139, the dislocation pit density is higher with CO_2 ON than with CO_2 OFF while the twin density is higher with CO_2 OFF than with CO_2 ON. The grain boundary length per unit area is also higher in run 17-139 with CO_2 ON than with CO_2 OFF. For run 17-143, however, the results are reversed. The dislocation pit density is higher with CO_2 OFF while the twin density is higher with CO_2 ON. There is no significant difference in the grain boundary length with or without CO_2. The various thermal and mechanical processes during the solidification process determine the type and concentration of structural defects.

The second batch[12] of EFG samples consisted of 13 wafers and a summary of the characterization results is given in Table 9. The dislocation pit density ranges from 8.7 E-03 to 3.8 E-02 pits per μm^2 with an average of 2.5 E-02 pits per μm^2 (2.6×10^6 pits per cm^2). The twin density ranges from 79.9 to 1441.1 lines per mm^2 with an average of 740.8 lines per mm^2. Finally, the grain boundary length ranges from 0.049 to 0.905 mm per mm^2, with an average of 0.273 mm per mm^2. The second batch of EFG samples had higher dislocation pit densities and twin densities than the first batch.

Photomicrographs are shown in Figures 4, 5, 6, and 7. These photomicrographs show the inhomogeneous distribution of defects on the EFG sample surface wherein defects tend to concentrate in certain areas, leaving large defect-free areas. They also show that many of the twin boundaries present are free from dislocation pile-up. According to Schwuttke[13], this type of twins are not electrically active and do not affect the conversion efficiency.

Large area (50 cm^2) cells have been fabricated from Run 17-143 as reported in reference 17. A total of nine cells were processed and tested. The average conversion efficiency was found to be 9.6% for a ribbon with 0.2% to 0.33% CO_2 applied to the growth catridge. Reference 17 also lists conversion efficiency to be 5.4% for cells fabricated from Run 17 - 139 without CO_2 in growth ambient. Higher efficiency of 7.3% was obtained for Run 17 - 139 with 0.23% CO_2 in growth ambient.

C. SOC Silicon Samples:

The twenty-three (23) Silicon-on-Ceramics[7] samples consisted of 19 flat samples and 4 side mounted specimens. The sample surface topography was very uneven due to irregular dendritic growth extending deep from the surface. The photomicrographs in Figures 8 and 9 show ridges and valleys which correspond to the dendritic growth. Enormous amounts of grain boundaries are present in these samples as shown in Figures 10 and 11. Figures 12 and 13 also show interactions between structural defects in the form of dislocations piling-up against twin and grain boundaries. These samples were characterized for dislocation pit density, twin density, and grain boundary length, and the results are summarized in Tables 10, 11 and 12, respectively.

This batch of SOC samples has a dislocation pit density that ranges from 5.9 E-03 to 7.0 E-02 pits per um^2, with an average of 1.8 E-02 pits per μm^2 (1.9×10^6 pits per cm^2). It has an average twin density of 778.3 lines per mm^2, with a range 533.2 to 1072.0 lines per mm^2. The average grain boundary length unit area is 11.84 mm per mm^2, with values ranging from 4.96 to 19.15 mm per mm^2.

D. Dendritic Web Silicon Samples:

Ten (10) Dendritic Web [6] samples were also received for characterization. The as-received sample surfaces were observed to be well polished and the samples were chemically etched without any chemical polishing. Optical examination of the prepared surfaces revealed that the only structural defects present in the plane of polish were dislocation pits. Therefore, these samples were analyzed for dislocation pits only.

The results of the dislocation pit density measurements are given in Table 13. The dendritic web samples have an average dislocation pit density of 2.8 E-04 pits per μm^2 (2.9×10^4 pits per cm^2), with a range of 1.8 E-04 to 5.7 E-04 pits per μm^2.

E. Step-Etching of Seven Samples:

MRI has also done step-etching [10] on seven solar cells, 3 from HAMCO and 4 EFG solar cell materials, and the results are shown in Tables 14-18. It is felt that the results are inconclusive at this stage and that several sources of errors may be present in the procedure used.

MRI is proposing to JPL that more step-etching tests be done using an improved procedure to insure reliability of results.

SECTION V

CONCLUSIONS

Given in Table 19 is the summary of all the characterization work done by MRI for JPL in the past contract period. The table shows the type of solar cell material, the number of samples analyzed, and the average defect densities obtained. Unfortunately, only five (5) of these 193 samples have actually been fabricated into solar cells and tested for their conversion efficiencies.

The results show that the dendritic web samples have a very low dislocation pit density of 2.87 E-04 pits per μm^2 which corresponds to 2.87×10^4 pits per cm^2. ASEC has measured conversion efficiencies on five of these cells and obtained an average conversion efficiency of 10.68%.

The single crystal HEM samples also have a low defect concentration. The samples have an average precipitate density of 5.1 E-03 precipitates per μm^2 (5.1×10^5 precipitates per cm^2). These single crystals may give relatively high conversion efficiencies because of their relatively low line defect concentration, however, the effect of the SiC precipitates is not known. The polycrystalline samples have added structural defects such as twin and grain boundaries as shown in Table 19, and their conversion efficiencies are expected to be lower. Dislocation pit densities of the order of 10^2 pits per cm^2 have also been observed on the HEM samples.

The Mobil Tyco EFG samples have a relatively higher defect density compared to the HEM or Web samples. The thirty-eight (38) samples have an overall average dislocation pit density of 1.939 E-02 pits per μm^2 (2×10^6 pits per cm^2). The average twin density is 461 lines per mm^2 and the average grain boundary length is 0.426 mm per mm^2. In Table 21, thirty-eight samples are divided into three classifications, on whether a CO_2 atmosphere was used. This information was not available on eighteen (18) samples. It is expected that slightly lower conversion efficiencies would be obtained from this type of solar cell material compared to either the Dendritic Web or the single crystal HEM samples, based only on the density of structural defects.

The use of a CO_2 atmosphere does not seem to have any significant effect on the surface defect densities as shown in Table 21. However, reports[14-17] show increased conversion efficiencies in runs with CO_2 ON. This enhancement may then be due to another mechanism that is independent of structural defect concentration.

The Silicon-on-Ceramics samples had the highest defect densities among all the samples. The samples have an average dislocation pit density of 1.86 E-02 pits per μm^2 (2×10^6 pits per cm^2), an average twin density of 778.3 lines per mm^2 which is much higher than the twin density for the EFG samples, and a grain boundary length of 11.8 mm per mm^2. The grain boundary length of the SOC samples is approximately 28 times larger than the grain boundary length of the EFG samples. The high concentration of structural defects and the interactions between these defects would result in lower conversion efficiencies.

It is suggested that all the above samples be processed into solar cells and tested for their conversion efficiencies. Then, an empirical relationship may be developed between the type and density of the defects and the conversion efficiency.

SECTION VI

REFERENCES

1. R. Natesh, H. A. Qidwai: "Quantitative Analysis of Defects in Silicon", One - Time Report on Crystal Etching Preparation Technique, DOE/JPL 954977, Materials Research, Inc., Technical Report: MRI - 259, 1978.

2. R. Natesh, J. M. Smith, T. Bruce, H. A. Qidwai: "Quantitative Analysis of Defects in Silicon", Final Report, DOE/JPL 954977, Materials Research, Inc., Technical Report: MRI - 276, 1980.

3. R. Natesh, J M. Smith: "Quantitative Analysis of Defects in Silicon", Monthly Technical Letter Progress Report No. 10, DOE/JPL 954977, Materials Research, Inc., Technical Report: MRI - 270, 1979.

4. R. Natesh, J. M. Smith, H. A. Qidwai, T. Bruce: "Quantitative Analysis of Defects in Silicon", Quarterly Progress Report, DOE/JPL 954977, Materials Research, Inc., Technical Report: MRI - 273, 1979.

5. E. Underwood, Quantitative Stereology, Addison - Wesley Publishing Co., Mass., 1970.

6. R. Natesh, M. Plichta, J. M. Smith: "Analysis of Defect Structure in Silicon", Informal Technical Report, DOE/JPL 955676, Materials Research, Inc., Technical Report: MRI - 280, 1980.

7. R. Natesh, M. Mena, J. M. Smith, M. A. Sellani: "Analysis of Defect Structure in Silicon", Characterization of Silicon - on-Ceramics Material, Informal Technical Report, DOE/JPL 955676, Materials Research, Inc., Technical Report: MRI - 281, 1981.

8. R. Natesh, M. Mena, J. M. Smith, M. A. Sellani: "Analysis of Defect Structure in Silicon", Mobil Tyco EFG Samples, Informal Technical Report, DOE/JPL 955676, Materials Research, Inc., Technical Report: MRI - 282, 1981.

9. R. Natesh, M. Mena, M. A. Sellani: "Analysis of Defect Structure in Silicon", Single Crystal and Polycrystalline HEM Material, Informal Technical Report, DOE/JPL 955676, Materials Research., Inc., Technical Report: MRI - 283., 1981.

10. R. Natesh, M. Mena, J. M. Smith, M. A. Sellani: "Analysis of Defect Structure in Silicon", Characterization of HAMCO and EFG Solar Cells, Informal Technical Report DOE/JPL 955676, Materials Research, Inc., Technical Report: MRI - 284, 1981.

11. R. Natesh, M. Mena, J. M. Smith, M. A. Sellani: "Analysis of Defect Structure in Silicon", Characterization of HEM Solar Cell Material, Informal Technical Report, DOE/JPL 955676, Materials Research, Inc., Technical Report: MRI - 285, 1981.

12. R. Natesh, M. Mena, J. M. Smith, M. A. Sellani: "Analysis of Defect Structure in Silicon", Characterization of Mobil Tyco EFG Sheet Material, Informal Technical Report, DOE/JPL 955676, Materials Research, Inc., Technical Report: MRI - 286, 1981.

13. G. H. Schwuttke, T. F. Ciszek, A. Kron: "Silicon Ribbon Growth by a Capillary Action Shaping Technique", Final Report, DOE/JPL 954144, IBM Corporation, 1977.

14. H. I. Yoo, P. A. Iles, D. C. Leung: "Silicon Solar Cell Process Development, Fabrication and Analysis", Seventh Quarterly Report DOE/JPL 955089, Optical Coating Laboratory, Inc., 1980.

15. F. V. Wald, et. al.: "Large Area Silicon Sheet by EFG", Fourth Quarterly Report, DOE/JPL 954355, Mobil Tyco Solar Energy Corporation, 1980.

16. J. P. Kalejs, et. al.: "Large Area Silicon Sheet by EFG", First Quarterly Report, DOE/JPL 954355, Mobil Tyco Solar Energy Corporation, 1981.

17. J.P. Kalejs: " Large Area Silicon Sheet by EFG ", Quarterly Report, January 1982, Mobil Tyco Solar Energy Corporation.

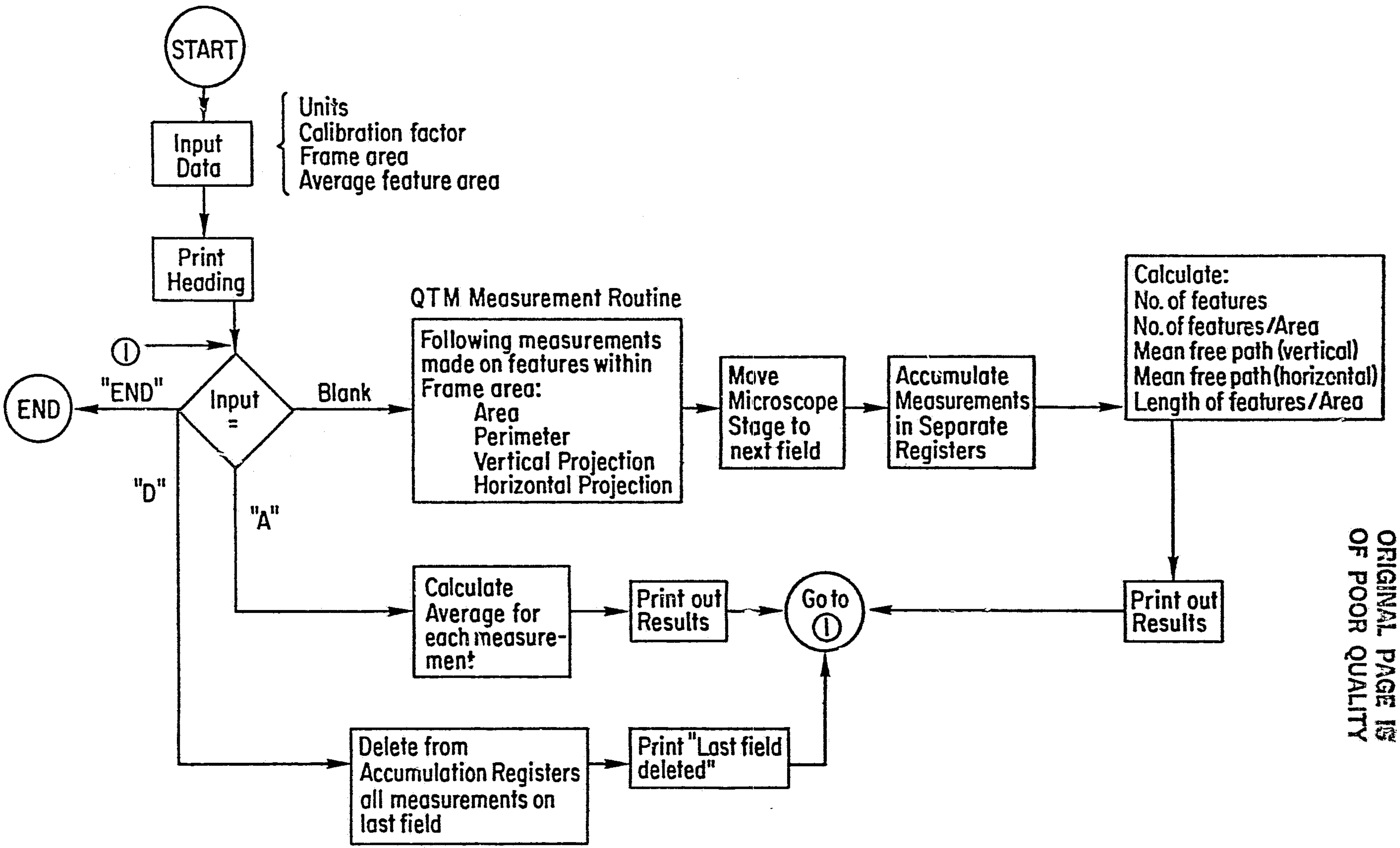

Figure 1. Basic Flowchart and Data Reduction Used in Defect Analysis

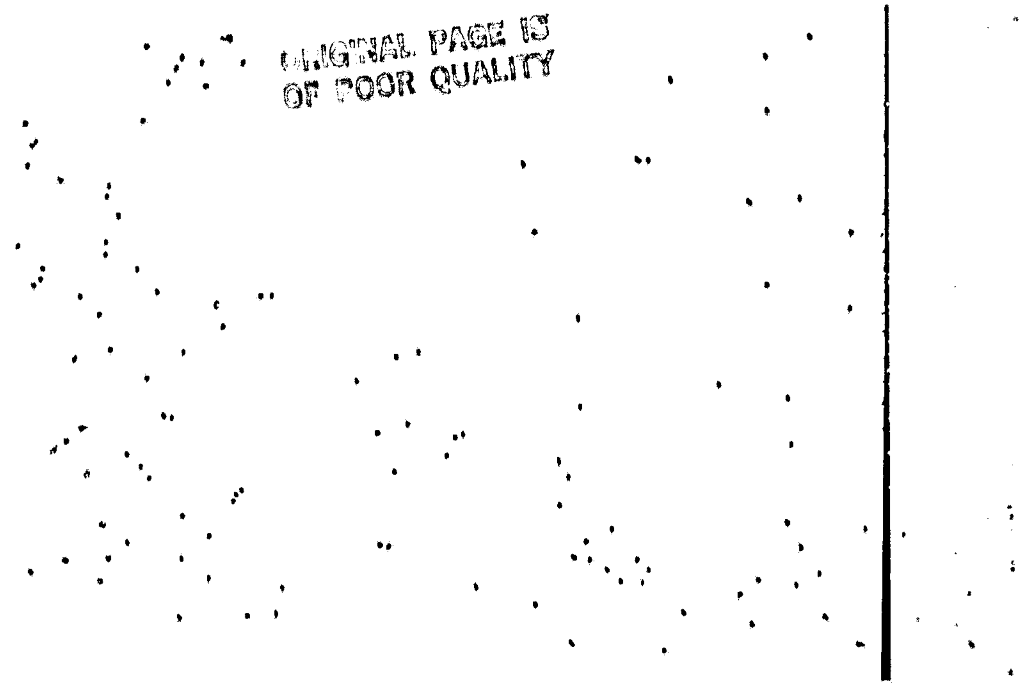

Figure 2. Silicon Carbide Precipitate Particles, HEM Sample (250X)

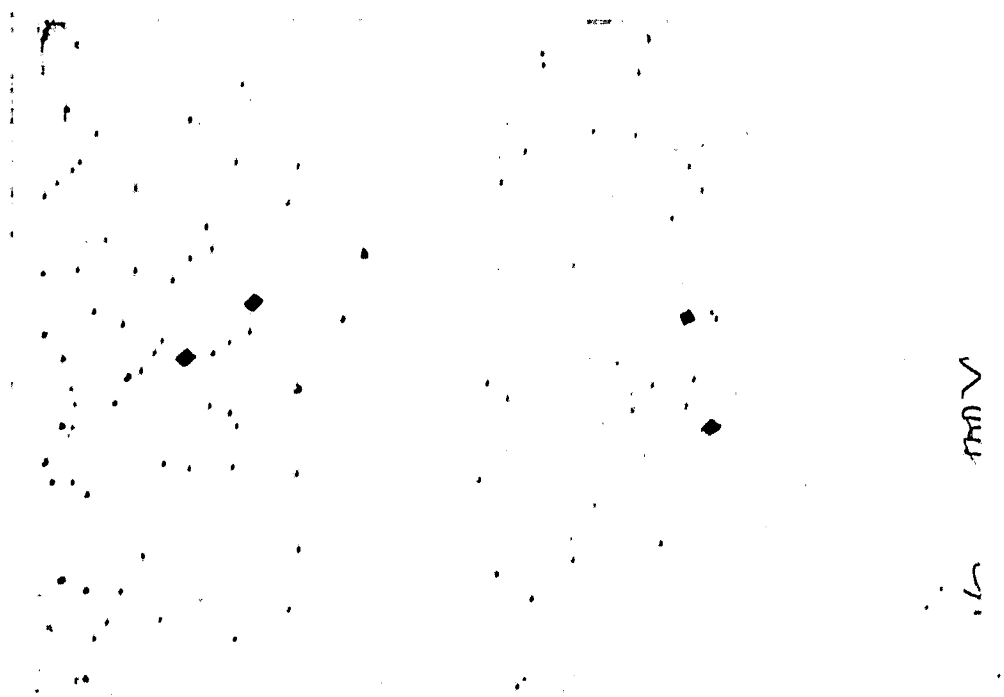

Figure 3. Dislocation Pits, HEM Sample (500X)

Figure 4. Region of High Twin Density, EFG Sample (200X)

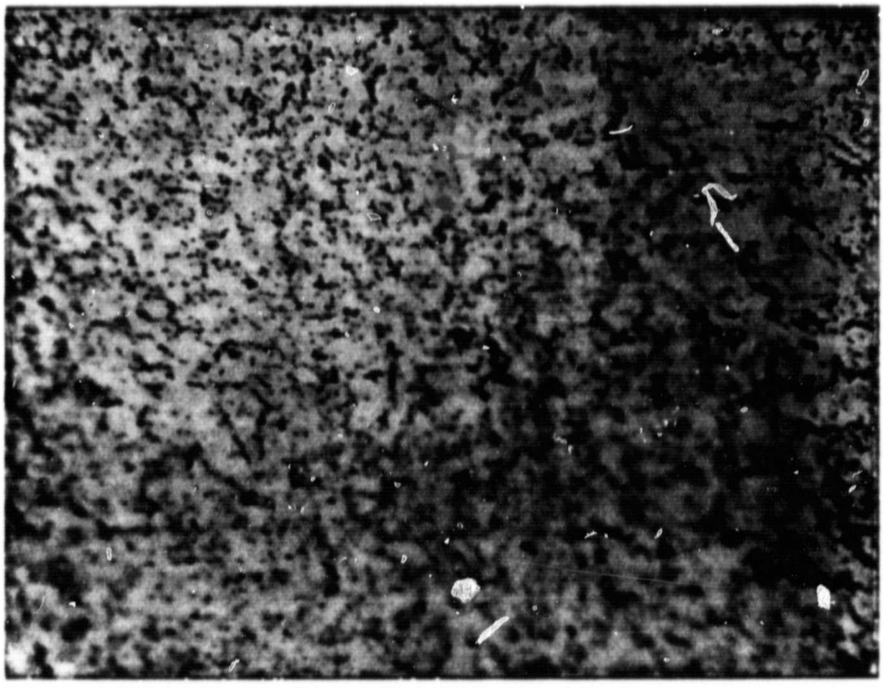

Figure 5. Region of High Dislocation Pit Density but no Twins, EFG Sample (200X)

ORIGINAL PAGE
BLACK AND WHITE PHOTOGRAPH

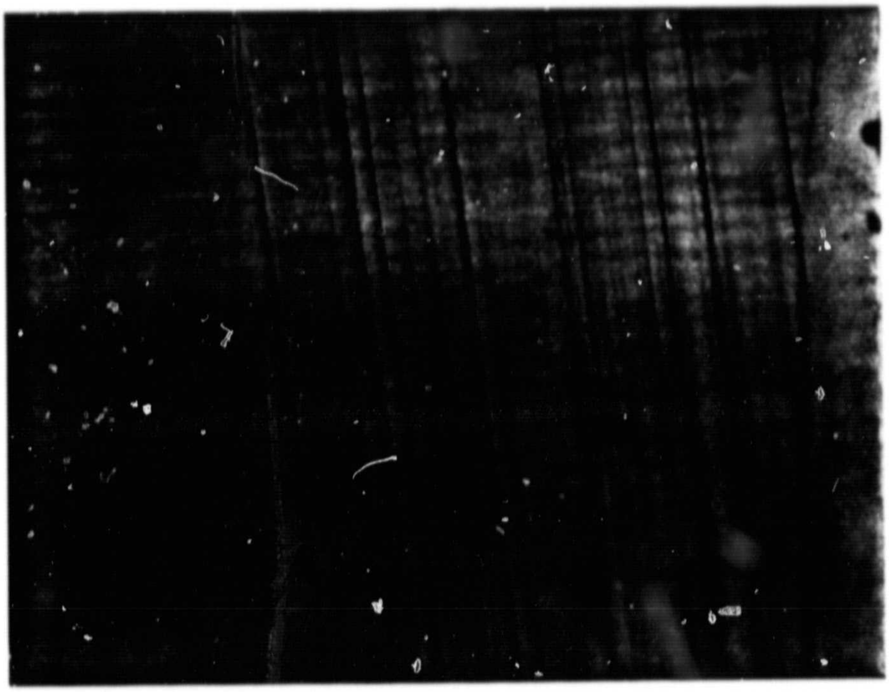

Figure 6. Twins Free from Dislocation Pile-up, EFG Sample (200X)

Figure 7. Twins with Dislocation Pile-up, EFG Sample (200X)

Figure 8. Dendritic Growth in SOC sample showing sharp changes in surface topography. (50X)

Figure 9. Higher magnification view of a region inside dendrites. (500 X)

Figure 10. Twins and Grain Boundaries, SOC Sample (75X)

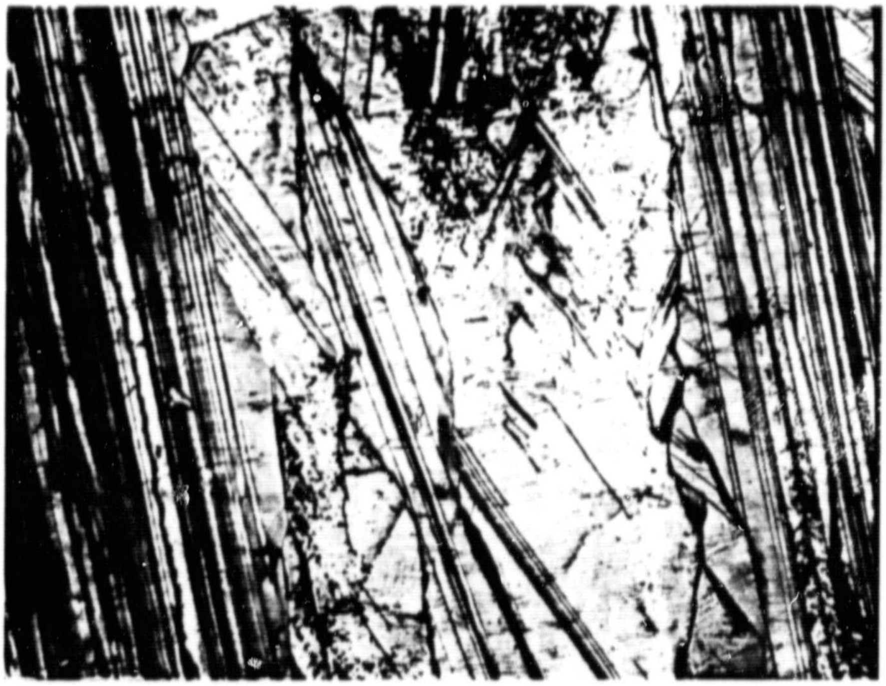

Figure 11. Grain Boundaries and Heavy Twinning, SOC Sample (100X)

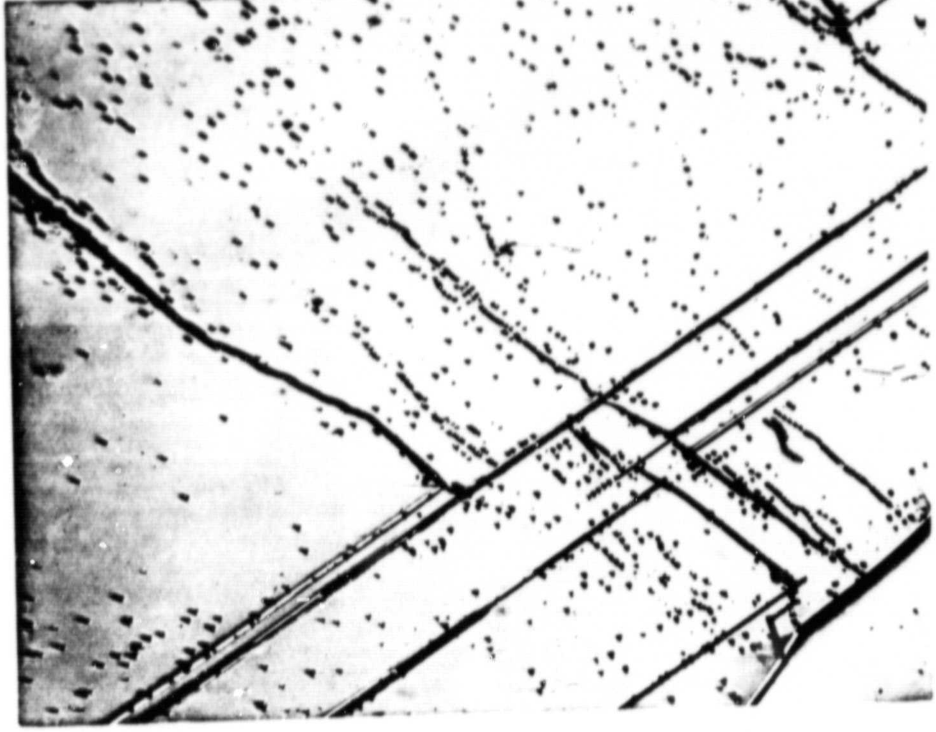

Figures 12 and 13. Dislocation Pile-up on Twin and Grain Boundaries, SOC Sample (500X)

TABLE 1

EQUATIONS FOR SYSTEMS OF LINES IN A PLANE [5]

Type of System	Isometric Lines, $(L_A)_{is}$ =	Oriented Lines $(L_A)_{or}$ =	Total Specific Line Length, L_A =
Isometric	$1.571\ P_L$	—	$1.571\ P_L$
Oriented	—	$(P_L)_{\perp}$	$(P_L)_{\perp}$
Partially Oriented	$1.571\ (P_L)_{\parallel}$	$(P_L)_{\perp} - (P_L)_{\parallel}$	$(P_L)_{\perp} + 0.571\ (P_L)_{\parallel}$

TABLE 2

CALIBRATION OF VIDEO DISPLAY ON THE OLYMPUS HBM MICROSCOPE

Grid Size is 11 x 11 cms.

Microscope Objective	Total Magnification	Length of Test Line	Area of Grid
10X	290X	.380 mm	.1444 mm^2
20X	580X	.190 mm	.0361 mm^2
40X	1100X	.100 mm	.0100 mm^2

TABLE 3

ANALYSIS OF HEM SINGLE CRYSTAL ("A") SAMPLES, WAFER NUMBERS: 4T-20, 4B-20, 3T-20, 3B-20, 103, 5 and 53

Sample Number	Precipitate Density precipitates per μm^2
A1	1.883 E-03
A2	6.095 E-03
A3	5.475 E-03
A5	4.367 E-03
A6	8.840 E-03
A7	9.910 E-03
A8	4.291 E-03
A9	8.336 E-03
A10	1.592 E-03
A11	7.585 E-03
A12	6.963 E-03
A13	6.673 E-03
A14	7.133 E-03
A15	1.159 E-03
A16	7.367 E-03
A17	1.159 E-03
A18	2.896 E-03
A19	2.387 E-03
A20	1.918 E-03
A21	3.802 E-03
A22	3.647 E-03
A23	2.589 E-03
A24	1.466 E-03
A25	1.503 E-02
Batch Average	5.149 E-03
SD	3.347 E-03

TABLE 4

ANALYSIS OF HEM POLYCRYSTALLINE ("B") SAMPLES, WAFER NUMBERS: 4T-20, 4B-20, 3T-20, 3B-20, 103, 5 and 53

Sample Number	Precipitate Density, precipitates per μm^2	Twin Density, lines per mm^2	Grain Boundary Length, mm per mm^2
B1	1.207 E-02	0.040	0.140
B2	1.088 E-02	0.011	0.314
B3	1.086 E-02	0.009	0.035
B4	8.741 E-03	0.011	0.070
B5	5.433 E-03	0.045	0.524
B6	3.717 E-03	0.045	0.524
B7	2.867 E-03	0.107	0.489
B8	1.697 E-03	0.027	0.175
B9	1.827 E-03	0	0
B10	2.170 E-03	0.174	0.838
B11	2.510 E-03	0.011	0.593
B12	2.024 E-03	0.113	0.454
B13	3.326 E-03	0.040	0.244
B14	1.987 E-03	0.071	0.244
B16	2.205 E-03	0.153	0.244
B17	3.275 E-03	0.017	0.035
B18	2.008 E-03	0.018	0.454
B19	2.575 E-03	0.061	0.279
B20	2.441 E-03	0.085	0.279
Batch Average	4.384 E-03	0.055	0.312
SD	3.490 E-03	0.051	0.222

TABLE 5

SUMMARY OF RESULTS FOR SEVENTY-TWO HEM SAMPLES

Sample Number	Dislocation Pit Density, pits per mm^2	Precipitate Density, precipitate per μm^2	Twin Density, lines per mm^2	Grain Boundary Length, mm per mm^2
1A2-1	1.667	1.990 E-03	0	0.022
1A2-2	1.951	1.954 E-03	0	0
1A2-3	3.333	3.102 E-03	3.059	0
2A2-5	1.442	2.058 E-03	1.413	0.201
2A2-6	1.456	2.480 E-03	39.716	0.254
1B4-1	2.691	5.194 E-03	15.425	0.117
1B4-2	1.844	2.615 E-03	0	0
1B4-L	0.997	2.417 E-03	0	0.052
2B4-1	0.699	3.700 E-03	2.454	0.419
2B4-2	3.320	5.173 E-03	4.153	0.838
2B4-3	5.590	3.157 E-03	16.848	0.445
3B4-1	1.404	1.670 E-03	0	0.055
3B4-2	1.185	2.919 E-04	0	0
4B10-1	1.361	1.329 E-03	8.105	0.150
4B10-2	1.014	1.162 E-02	9.315	0.273
4B10-3	0.787	6.078 E-03	22.735	0.144
7B8-1	4.000	3.231 E-03	16.286	0.489
7B8-2	6.444	2.113 E-03	27.378	0.524
7B8-3	2.667	1.417 E-03	23.449	0.419
7B8-5	2.000	9.775 E-04	38.777	0.349
7B8-6	4.222	1.892 E-03	68.868	0.489
7B8-7	10.222	1.914 E-03	0	0.070
7B8-9	4.889	1.657 E-03	13.752	0.454
7B8-10	2.167	4.135 E-03	1.539	0.131
7B8-11	5.882	9.044 E-04	7.989	0.334

TABLE 5 CONTINUED

SUMMARY OF RESULTS FOR SEVENTY-TWO HEM SAMPLES

Sample Number	Dislocation Pit Density, pits per mm^2	Precipitate Density, precipitates per μm^2	Twin Density, lines per mm^2	Grain Boundary Length, mm per mm^2
7B8-13	2.220	1.268 E-03	16.357	0.175
7B8-14	2.764	1.676 E-03	5.471	0.230
7B8-15	1.667	1.103 E-03	4.024	0.183
1C4-1	0.699	1.068 E-03	7.497	0.100
1C4-2	1.570	3.132 E-03	24.226	0.648
1C4-3	2.100	2.596 E-03	17.969	0.449
2C4-1	6.110	2.831 E-03	2.430	0.937
2C4-2	9.260	4.958 E-03	4.575	0.541
2C4-3	0.349	1.683 E-03	8.266	0.604
3C8-1	4.651	1.486 E-03	1.887	0.268
3C8-2	4.167	3.111 E-03	23.491	0.491
3C8-3	2.667	1.094 E-03	19.943	0.524
3C8-5	2.862	1.612 E-03	4.315	0.476
3C8-6	2.299	3.020 E-03	20.610	0.645
4C4-1	0.524	1.398 E-03	12.778	0.209
4C4-2	1.050	2.099 E-03	6.783	0.105
4C4-3	0.349	6.616 E-04	7.957	0.279
7M2-2	8.673	6.368 E-03	1.017	0.267
7M2-3	3.876	9.221 E-03	1.987	0.950
7M2-4	3.182	1.504 E-03	24.352	0.571
7M2-6	3.684	4.726 E-03	0	0.110
7M2-7	3.158	3.096 E-03	3.463	0.165
7M2-8	2.444	1.282 E-02	10.866	0.559
7M2-10	2.889	7.483 E-03	3.547	0.349
7M2-11	2.889	5.546 E-03	0	0.035

TABLE 5 CONTINUED

SUMMARY OF RESULTS FOR SEVENTY-TWO HEM SAMPLES

Sample Number	Dislocation Pit Density, pits per mm^2	Precipitate Density, precipitates per μm^2	Twin Density, lines per mm^2	Grain Boundary Length, mm per mm^2
7M2-12	8.889	3.373 E-03	6.117	0.454
7M2-14	25.556	8.467 E-03	19.441	0.803
7M2-15	4.444	6.644 E-03	12.595	0.384
7M2-16	3.556	3.281 E-03	0	0.244
7M2-19	11.000	3.407 E-03	17.745	0.244
7T7-1	4.127	3.299 E-03	7.976	0.150
7T7-2	6.667	2.434 E-03	11.208	0.224
7T7-3	3.167	4.571 E-03	31.734	0.340
7T7-4	2.857	8.647 E-03	24.571	0.324
7T7-5	3.167	4.389 E-03	50.215	0.419
7T7-6	1.789	4.608 E-03	124.943	0.230
7T7-7	1.754	3.854 E-03	23.412	0.138
7T7-8	5.200	7.654 E-03	25.003	0.128
7T7-9	3.758	3.507 E-03	49.668	0.282
7T7-10	3.454	4.818 E-03	28.845	0.217
7T7-11	4.615	1.804 E-03	46.132	0.242
7T7-12	3.810	2.307 E-03	88.872	0.474
9A7-1	2.763	7.390 E-03	1.884	0.145
9A7-2	0.524	1.805 E-03	1.355	0.105
9A7-3	15.700	3.060 E-03	39.560	0.663
9A7-4	4.540	1.879 E-03	6.869	0.419
9A7-5	1.750	6.101 E-03	10.195	0.079
Average	3.752	3.482 E-03	16.437	0.315

TABLE 6

WAFER AVERAGES FOR SEVENTY-TWO HEM SAMPLES

Wafer Number	Dislocation Pit Density, pits per mm^2	Precipitate Density, precipitates per μm^2	Twin Density, lines per mm^2	Grain Boundary Length, mm per mm^2
1A2	2.317	2.349 E-03	1.170	0.007
2A2	1.449	2.269 E-03	20.565	0.228
1B4	1.844	3.409 E-03	5.142	0.056
2B4	3.203	4.010 E-03	7.818	0.567
3B4	1.295	9.810 E-03	0	0.028
4B10	1.054	2.856 E-03	13.385	0.189
7B8	3.929	1.861 E-03	18.658	0.321
1C4	1.456	5.469 E-03	16.564	0.399
2C4	5.240	1.670 E-03	5.090	0.694
3C8	3.329	2.065 E-03	14.049	0.466
4C4	0.641	1.386 E-03	9.053	0.193
7M2	6.480	5.841 E-03	7.779	0.392
7T7	3.697	4.324 E-03	42.714	0.264
9A7	5.037	4.047 E-03	11.973	0.282

TABLE 7

ANALYSIS OF MOBIL-TYCO EFG SAMPLES

Sample Number	Dislocation Pit Density, per μm^2	Twin Density, per mm^2	Grain Boundary Length, mm/mm^2
EFG 17-139-A	1.545 E-02	453.553	0.568
(CO_2 OFF) B	1.264 E-02	403.335	0.171
C	7.337 E-03	1192.780	0.114
D	2.490 E-02	179.962	0.229
E	4.632 E-03	695.013	-
EFG 17-139-F	2.070 E-02	144.057	0.514
(CO_2 ON) G	3.292 E-02	204.798	0.600
H	9.712 E-03	322.519	0.379
I	7.616 E-03	96.891	0.400
J	1.597E-02	295.899	0.947
EFG 17-143-A	3.022 E-02	499.521	0.189
(CO_2 OFF) B	1.415 E-02	611.570	1.326
C	2.219 E-02	289.859	0.253
D	1.346 E-02	228.574	0.286
E	1.530 E-02	368.724	0.540
EFG 17-143-F	8.796 E-03	473.206	0.180
(CO_2 ON) G	8.673 E-03	763.666	0.267
H	1.773 E-02	349.726	0.293
I	1.887 E-02	331.244	0.706
J	2.379 E-02	354.361	1.123
EFG 17-146-A	2.824 E-02	229.454	0.960
B	3.130 E-02	460.619	0.253
C	3.503 E-02	165.054	0.424
D	1.253 E-02	381.455	0.112
E	2.283 E-02	218.708	0.884

TABLE 8

BATCH AVERAGES OF MOBIL - TYCO SAMPLE MEASUREMENTS

Batch Number	Dislocation Pit Density, per μm^2	Twin Density, per mm^2	Grain Boundary Length, mm/mm^2
EFG 17-139 (CO_2 OFF)			
a) Average	1.299 E-02	584.929	0.271
b) SD	7.903 E-03	385.952	0.284
EFG 17-139 (CO_2 ON)			
a) Average	1.738 E-02	212.833	0.568
b) SD	1.011 E-02	96.395	0.230
EFG 17-143 (CO_2 OFF)			
a) Average	1.906 E-02	399.650	0.519
b) SD	7.141 E-03	155.854	0.471
EFG 17-143 (CO_2 ON)			
a) Average	1.557 E-02	454.441	0.514
b) SD	6.644 E-03	181.749	0.392
EFG 17-146			
a) Average	2.599 E-02	291.058	0.527
b) SD	8.748 E-03	124.327	0.378

TABLE 9

SUMMARY OF DISLOCATION PIT DENSITY, TWIN DENSITY, AND GRAIN BOUNDARY LENGTH MEASUREMENTS FOR THE MOBIL TYCO EFG SAMPLES

(Runs 17 - 090 and 217 - 4D)

Sample Number	Dislocation Pit Density, per μm^2	Twin Density per mm^2	Grain Boundary Length, mm/mm^2
JPL 5-1459-A1	1.834 E-02	741.888	0.182
JPL 5-1459-B1	3.412 E-02	306.540	0.136
JPL 5-1459-C1	1.951 E-02	1142.460	0.143
JPL 5-1459-D1	8.777 E-03	750.317	0.190
JPL 5-1459-E1	1.026 E-02	747.730	0.150
JPL 5-1459-F1	2.226 E-02	638.795	0.182
JPL 5-1459-G1	2.692 E-02	464.212	0.087
JPL 5-1459-H1	1.275 E-02	1441.190	0.045
JPL 5-1459-I1	7.798 E-02	1044.880	0.143
JPL 5-1459-J1	2.617 E-02	850.496	0.571
JPL 5-1508-F	2.005 E-02	864.541	0.905
JPL 5-1508-G	1.609 E-02	558.001	0.409
JPL 5-1508-J	3.865 E-02	79.940	0.400
Batch Average	2.553 E-02	740.845	0.273

TABLE 10

ANALYSIS OF HONEYWELL SAMPLES, SOC RUN 195 - DISLOCATION DENSITY

Sample Number	Number Of Fields Taken	Average Dislocation Density, pits per μm^2
B2	0[b]	—
B3	10	1.5013 E-02
B4	25	2.1918 E-02
D2	3[a]	8.7300 E-03
D3	5[a]	1.3280 E-02
D4	25	1.2532 E-02
H1L	5[a]	7.0180 E-02
H1R	5	7.1800 E-03
H2L	25	9.4530 E-03
H2R	25	1.7050 E-02
H5L	25	5.9459 E-03
H5R	36	9.2352 E-03
T1L	10	1.2229 E-02
T1R	10	2.4692 E-02
T2L	26	7.6482 E-03
T2R	36	7.6761 E-03
T5L	25	7.8268 E-03
T5R	25	1.0575 E-02
M	16	6.9893 E-03
B5E	4[a]	3.8191 E-02
B1E	3[a]	2.4200 E-02
D5E	4[a]	3.4410 E-02
ME	4[a]	5.2938 E-02
Average		1.864 E-02

a - Measured Manually

b - No Silicon on surface

TABLE 11

ANALYSIS OF HONEYWELL SAMPLES, SOC RUN 195 - TWIN DENSITY

Sample Number	Number Of Fields Taken	Average Twin Density (per mm^2)	Standard Deviation	Relative Error at 90% Confidence (%)
B2	0[a]			
B3	18[b]	909.5106	202.3057	9.12
B4	31	624.6091	319.2008	15.10
D2	5[b]	897.3880	166.5779	17.70
D3	12[b]	978.7627	236.6235	12.53
D4	32	822.3684	317.5137	11.23
H1L	10[b]	808.8643	427.8349	30.66
H1R	10[b]	1072.0222	267.3229	14.45
H2L	32	568.7327	430.6487	22.02
H2R	32	801.0285	373.5975	13.56
H5L	32	533.2410	192.1538	10.48
H5R	32	624.1343	244.1130	10.86
T1L	32[b]	625.0000	304.8766	14.19
T1R	32[b]	1034.4529	269.6022	7.58
T2L	32	892.4861	432.0150	14.08
T2R	32	654.4321	306.0798	13.60
T5L	32	719.3560	315.9518	12.77
T5R	32	909.7992	430.8287	13.77
M	32	534.1066	336.8394	18.32
Average		778.3500		

a - All the Silicon has been etched out

b - Plenty of uncovered areas

TABLE 12

ANALYSIS OF HONEYWELL SAMPLES V-00578 - GRAIN BOUNDARY LENGTH

Sample Number	Number Of Fields Taken	Average Grain Boundary Length (mm/mm^2)	Standard Deviation	Relative Error at 90% Confidence (%)
B2	0[a]	—	—	—
B3	18[b]	16.7611	5.8463	14.31
B4	31	9.0151	4.9943	16.37
D2	5[b]	15.8789	3.8895	23.35
D3	12[b]	15.0850	2.7503	9.45
D4	32	13.5962	7.4908	16.02
H1L	10[b]	10.4801	3.6823	20.37
H1R	10[b]	13.9735	2.6781	11.11
H2L	32	6.5501	3.6910	16.39
H2R	32	6.4508	3.8250	17.24
H5L	32	7.9395	2.9084	10.65
H5R	32	9.4281	4.4537	13.74
T1L	32[b]	19.1540	6.2214	9.45
T1R	32[b]	17.2684	4.7680	8.03
T2L	32	13.3979	4.6152	10.02
T2R	32	10.7183	4.4731	12.14
T5L	32	9.3289	5.0335	15.69
T5R	32	13.1994	5.5366	12.20
M	32	4.9622	3.9466	23.13
Average		11.8440		

a - All the Silicon has been etched out

b - Plenty of uncovered areas

TABLE 13

ANALYSIS OF WESTINGHOUSE SAMPLES

JPL Sample Number	No. of Dislocations pits per field	No. of Dislocations pits per μm^2
J250-4.7-A	17.808	2.737×10^{-4}
J250-4.7-B	14.946	2.298×10^{-4}
J250-4.7-C	12.146	1.867×10^{-4}
J250-4.7-D	16.614	2.554×10^{-4}
J250-4.7-E	15.526	2.387×10^{-4}
J250-4.7-F	15.800	2.429×10^{-4}
J250-4.7-K_1	15.828	2.433×10^{-4}
J250-4.7-K_2	16.615	2.554×10^{-4}
J250-4.7-L_1	37.424	5.753×10^{-4}
J250-4.7-L_2	27.082	3.702×10^{-4}

TABLE 14

STEP - ETCHING OF SOLAR CELL EFG - 3

Etch Number	Surface Analyzed	Distance from Original Surface mils	Dislocation Pit Density, pits per μm^2	Twin Density, lines per mm^2	Grain Boundary Length, mm per mm^2
1	Top	0	—	71.982	0.240
2	Top	0.75	1.315 E-02	317.080	0.240
	Bottom	0.75	9.114 E-02	168.144	0.240
3	Top	1.55	3.224 E-02	72.632	0.240
	Bottom	1.55	3.930 E-02	40.027	0.240

TABLE 15

STEP - ETCHING OF SOLAR CELL EFG - 13

Etch Number	Surface Analyzed	Distance From Original Surface, mils	Dislocation Pit Density, pits per μm^2	Twin Density, lines per mm^2	Grain Boundary Length mm per mm^2
1	Top	0	—	322.892	0.060
2	Top	0.75	1.888 E-02	636.844	0.060
	Bottom	0.75	4.450 E-02	542.678	0.060
3	Top	2.45	3.414 E-02	1172.860	0.060
	Bottom	2.45	2.746 E-02	475.622	0.060

TABLE 16

STEP - ETCHING OF SOLAR CELL EFG - 31

Etch Number	Surface Analyzed	Distance From Original Surface mils	Dislocation Pit Density, pits per um^2	Twin Density lines per mm^2	Grain Boundary Length, mm per mm^2
1	Top	0	-	567.258	1.020
2	Top	0.40	1.974 E-02	459.326	1.020
	Bottom	0.40	3.247 E-02	319.204	1.020

TABLE 17

STEP - ETCHING OF SOLAR CELL EFG - 33

Etch Number	Surface Analyzed	Distance From Original Surface, mils	Dislocation Pit Density, pits per μm^2	Twin Density, lines per mm^2	Grain Boundary Length, mm per mm^2
1	Top	0	-	207.833	0.180
2	Top	1.25	2.227 E-02	386.874	0.180
	Bottom	1.25	4.324 E-02	190.946	0.180
3	Top	2.50	2.012 E-02	382.469	0.180
	Bottom	2.50	1.425 E-02	339.582	0.180

TABLE 18

STEP-ETCHING OF SOLAR CELL HAMCO 101 - 1

Etch Number	Surface Analyzed	Distance from Original Surface mils	Precipitate Density, precipitates per μm^2	Twin Density, lines per mm^2	Grain Boundary Length, mm per mm^2
1	Top	0	0	0	0
2	Top	1.10	0	0	0
	Bottom	1.10	0	0	0
3	Top	3.10	3.076 E-04	0	0
	Bottom	3.10	5.006 E-04	0	0

TABLE 19

STEP - ETCHING OF SOLAR CELL HAMCO 101 - 4

Etch Number	Surface Analyzed	Distance from Original Surface, mils	Precipitate Density, precipitates per μm^2	Twin Density, lines per mm^2	Grain Boundary Length, mm per mm^2
1	Top	0	0	10.145	0
2	Top	0.90	0	0	0
	Bottom	0.90	0	0	0
3	Top	1.80	3.438 E-03	0	0
	Bottom	1.80	3.965 E-03	0	0

TABLE 20

STEP-ETCHING OF SOLAR CELL HAMCO 108 - 1

Etch Number	Surface Analyzed	Distance from Original Surface, mils	Precipitate Density, precipitates per μm^2	Twin Density, lines per mm^2	Grain Boundary Length, mm per mm^2
1	Top	0	0	0	0
2	Top	0.80	0	0	0
	Bottom	0.80	0	0	0
3	Top	1.55	3.042 E-03	0	0
	Bottom	1.55	5.375 E-03	0	0

TABLE 21

ANALYSIS OF DEFECTS IN SILICON: SUMMARY

Coupon Type	Number of Coupons	Dislocation Pit Density, pits per μm^2	Precipitate Density, precipitates per μm^2	Twin Density, lines per mm^2	Grain Boundary Length, mm per mm^2	Conversion Efficiency %
HEM						
a) Single Crystal	24	*	5.149 E-03	0	0	
b) Polycrystal						
i) Batch 1	19	*	4.384 E-03	0.055	0.312	
ii) Batch 2	72	3.752 E-06	3.482 E-03	16.437	0.315	
EFG						
a) CO_2 ON	10	1.648 E-02	0	333.637	0.541	
b) CO_2 OFF	10	1.603 E-02	0	492.290	0.395	
c) Unclassified	18	2.566 E-02	0	615.904	0.344	
Silicon-on-Ceramics	23	1.864 E-02	0	778.350	11.844	
Dendritic Web	10	2.871 E-04	0	0	0	10.68

* - Not Measured
N. A. - Data Not Available

APPENDIX I

QTM 720 TELETYPE PRINTOUTS

ORIGINAL PAGE IS
OF POOR QUALITY

TT!=DX1!EFGE.DAT
DEFECTS IN SILICON(VERSION 3-8/1/79)

EFG-E 17-139 DISLOCATION PITS

OPERATOR IS JMSJMS MAGNIFICATION=X800
UNITS= MICRONS CALIBRATION FACTOR (UNITS/PP)= .3407
FRAME AREA= 160000 QTM OUTPUT WAS DIVIDED BY 1 AND CORRECTED
AVERAGE FEATURE AREA (PP)= 33.37

FLD	NO.	NO./AREA	MFPV	MFPH	L/A
1	150.614	8.10965E-03	52.7195	42.6875	.0349281
2	135.181	7.27868E-03	47.3194	49.5113	.0335981
3	64.3093	3.46266E-03	100.022	93.5026	.0164734
4	0	0	0	0	
5	0	0	0	0	
6	154.6	8.32425E-03	45.4267	41.2033	.037689
7	120.018	6.46223E-03	58.1772	58.0532	.0291312
8	26.401	1.42153E-03	365.852	375.945	4.46691E-03
9	92.4183	4.97616E-03	83.6074	82.845	.0195828
10	138.867	7.47714E-03	49.3321	47.8595	.0339467
11	12.8259	6.90595E-04	432.635	412.97	3.83402E-03
12	44.9805	2.42192E-03	169.292	158.006	.0100895
13	116.152	6.25408E-03	46.9526	46.1966	.0347446
14	6.29308	3.38843E-04	851.75	825.939	1.94453E-03
15	1.16871	6.29280E-05	4542.67	2595.81	8.07162E-04
16	219.718	.0118305	29.8369	28.3917	.0567673
17	128.019	6.89304E-03	71.8208	22.2135	.0369185
18	46.9883	2.53003E-03	272.56	112.628	.0122175
19	120.977	6.51386E-03	72.2971	57.9299	.0262603
20	28.5886	1.53932E-03	326.419	293.075	5.08145E-03
21	.988912	5.32468E-05	3206.59	37.5169	5.26490E-03
22	3.86575	2.08147E-04	2477.82	3634.13	5.31993E-04
23	23.674	1.27470E-03	1267.72	825.939	1.62350E-03
24	131.975	7.10603E-03	44.8289	46.9526	.0363223
25	101.438	5.46183E-03	59.1236	58.8682	.0288652
26	6.62272	3.56592E-04	370.83	336.494	1.96287E-03
27	223.254	.0120209	28.9649	25.3662	.0605188
28	46.6886	2.51389E-03	138.355	83.7358	.0129421
29	77.8843	4.19359E-03	123.61	80.7585	.0171614
30	356.278	.0191834	28.5852	21.4953	.0670953

*******AVERAGE*******

	NO.	NO./AREA	MFPV	MFPH	L/A
	86.0264	4.63199E-03	85.3662	66.2411	.0210257
SD	81.9149	4.41061E-03			.0189511
SE	14.9555	8.05264E-04			3.45999E-03

*

TT:=DX1:EFGET.DAT
DEFECTS IN SILICON(VERSION 3-8/1/79)

EFG-E 17-139 TWINS

OPERATOR IS JMS MAGNIFICATION=X800
UNITS= MM CALIBRATION FACTOR (UNITS/PP)= 3.40700E-04
FRAME AREA= 160000 QTM OUTPUT WAS DIVIDED BY 1 AND CORRECTED
AVERAGE FEATURE AREA (PP)= 2804

FLD	NO.	NO./AREA	MFPV	MFPH	L/A
1	27.4686	1479.02	.0223044	8.03064E-03	148.802
2	15.428	830.7	.085442	.0135636	79.0652
3	16.235	874.155	.0765618	.011198	96.6393
4	14.689	790.913	.144979	.0268136	41.5597
5	25.785	1388.36	.0626575	.0211205	61.8763
6	1.82703	98.3744	.345013	.0679701	15.7672
7	.879101	47.3342	.263343	.142329	9.11726
8	3.65549	196.826	.265912	.0337954	31.25
9	42.5685	2292.05	.0442467	8.95107E-03	116.451
10	5.4005	290.783	.109462	.0323513	33.6898
11	5.76427	310.37	.231966	.0339005	31.195
12	22.939	1235.12	.0287208	8.82357E-03	126.183
13	21.4654	1155.78	.0521147	.0130818	76.2676
14	9.73395	524.113	.0707948	9.76393E-03	107.82
15	14.5649	784.23	.0256165	.0103047	126.202
16	5.98787	322.41	.196086	.027629	58.2991
17	5.84237	314.575	.091005	.022025	49.9064
18	4.35164	234.309	.0916168	.0254135	39.1657
19	6.91084	372.106	.0570806	.0149553	74.4882
20	1.37019	73.776	1.11249	.13628	7.76893
21	4.9975	269.085	.114281	.0247557	43.6601
22	26.1002	1405.34	.0607038	.0128173	79.7347
23	11.7668	633.567	.176414	.027338	39.3767
24	20.7418	1116.82	.0761341	.0151886	71.232
25	6.07275	326.98	.20727	.0388262	27.8012
26	7.73395	416.425	.0548963	.0143793	79.8173
27	11.408	614.25	.0315646	.0182071	69.2416
28	8.99108	484.114	.0779857	.0255445	44.2013
29	4.07347	219.331	.0574415	.0271339	37.8082
30	32.4864	1749.19	.0209581	8.47644E-03	144.941

********AVERAGE********

	NO.	NO./AREA	MFPV	MFPH	L/A
	12.908	695.013	.0640689	.0171913	65.6443
SD	10.1934	548.851			38.5276
SE	1.86105	100.206			7.03415

*

TT:=DX1:JPLH5R.DAT
DEFECTS IN SILICON(VERSION 3-8/1/79)

JPLH5R (DISL. PIT DENSITY) Silicon-on-Ceramics

OPERATOR IS JMS MAGNIFICATION=X800
UNITS= MM CALIBRATION FACTOR (UNITS/PP)= 3.40700E-04
FRAME AREA= 160000 QTM OUTPUT WAS DIVIDED BY 1 AND CORRECTED
AVERAGE FEATURE AREA (PP)= 13.01

FLD	NO.	NO./AREA	MFPV	MFPH	L/A
1	450.961	24281.4	.0484551	.0454645	33.167
2	10.761	579.411	3.20659	.50011	1.26578
3	249.116	13413.4	.077322	.0772125	20.8028
4	244.197	13148.5	.0702474	.0690025	22.1878
5	222.137	11960.7	.0998388	.0834793	23.5086
6	93.6203	5040.87	.153555	.149348	9.97946
7	132.821	7151.58	.141223	.108159	12.0524
8	96.618	5202.28	.16321	.17528	9.46581
9	249.5	13434.1	.0704289	.0708869	23.0316
10	242.198	13040.9	.0631657	.0618751	26.1777
11	154.573	8322.82	.0853083	.0581772	20.1148
12	104.919	5649.26	.155305	.0976917	17.464
13	135.895	7317.13	.144979	.0779857	15.0059
14	364.105	19604.8	.0548963	.0508507	30.8464
15	68.7164	3699.95	.251207	.209662	7.20942
16	274.251	14766.7	.0593166	.0547594	29.7549
17	79.1699	4262.81	.186048	.193993	8.88795
18	104.151	5607.87	.13731	.178144	10.7408
19	132.052	7110.2	.132956	.121408	13.4558
20	235.665	12689.1	.0845147	.0639062	20.5643
21	500.538	26950.9	.0326224	.0279692	53.5662
22	24.5196	1320.23	.524154	.561979	2.81589
23	83.4743	4494.57	.208858	.196794	7.96155
24	103.228	5558.21	.194686	.148534	8.99802
25	66.6411	3588.21	.356288	.334429	4.51277
26	31.2836	1684.43	.767775	.567833	2.36645
		*******AVERAGE*******			
	NO.	NO./AREA	MFPV	MFPH	L/A
	171.35	9226.16	.103749	.0904763	16.7655
SD	123.714	6661.23			11.5872
SE	24.2623	1306.37			2.27245
27	6.37971	343.508	1.06886	1.11249	1.80694
28	219.985	11844.8	.129175	.101512	14.2996
29	151.806	8173.83	.133608	.162238	10.007
30	362.798	19534.4	.0600352	.0456549	31.782
31	464.412	25005.7	.0465914	.0420293	37.3221
32	101.845	5483.71	.190601	.0959718	12.5569
33	133.205	7172.28	.17528	.0846459	15.9139
34	43.4281	2338.34	.44682	.450512	3.7423
35	109.685	5905.85	.19127	.108374	12.2267
36	125.98	6783.24	.171421	.0805199	19.0967
		*******AVERAGE*******			
	NO.	NO./AREA	MFPV	MFPH	L/A
	171.518	9235.17	.109376	.0908912	16.5183
SD	126.814	6828.14			11.3362
SE	21.1357	1138.02			1.88936

*

ORIGINAL PAGE IS
OF POOR QUALITY

TT!=DX1!WEBL2.DAT
DEFECTS IN SILICON(VERSION 3-8/1/79)

250J-4.7-L2

OPERATOR IS MRP MAGNIFICATION=32X
UNITS= MICRONS CALIBRATION FACTOR (UNITS/PP)= .3607
FRAME AREA= 500000 QTM OUTPUT WAS DIVIDED BY 1 AND CORRECTED
AVERAGE FEATURE AREA (PP)= 27.36

FLD	NO.	NO./AREA	MFPV	MFPH	L/A
1	101.17	1.55521E-03	335.847	322.054	5.39784E-03
2	48.4649	7.45015E-04	665.498	653.442	2.53673E-03
3	42.7632	6.57366E-04	733.13	724.297	2.26227E-03
4	32.6389	5.01734E-04	954.233	1013.2	1.79096E-03
5	19.0424	2.92725E-04	1478.28	1490.5	1.14777E-03
6	25.402	3.90487E-04	1235.27	1420.08	1.33075E-03
7	28.8012	4.42739E-04	1024.72	1030.57	1.77433E-03
8	19.1155	2.93848E-04	1568.26	1568.26	1.10341E-03
9	11.8056	1.81478E-04	2540.14	2732.58	6.82007E-04
10	8.66228	1.33159E-04	2774.62	3402.83	5.76657E-04
11	10.4532	1.60690E-04	2282.91	1939.25	7.92903E-04
12	7.89474	1.21360E-04	4098.86	3920.65	3.77045E-04
13	2.11988	3.25874E-05	10608.8	12023.3	1.55254E-04
14	4.16667	6.40511E-05	5465.15	5465.15	3.04963E-04
15	2.26608	3.48348E-05	8197.73	8197.73	3.57638E-04
16	2.37573	3.65204E-05	10608.8	9492.1	1.55254E-04
17	8.55263	1.31473E-04	2691.79	3757.29	4.51899E-04
		********AVERAGE********			
	NO.	NO./AREA	MFPV	MFPH	L/A
	22.0997	3.39722E-04	1382.93	1396.15	1.24692E-03
SD	24.0954	3.70400E-04			1.25934E-03
SE	5.84398	8.98352E-05			3.05436E-04
18	109.539	1.68387E-03	280.919	299.088	5.99390E-03
19	69.9927	1.07595E-03	444.212	442.034	3.86471E-03
20	51.6813	7.94458E-04	658.212	644.107	2.56446E-03
21	27.3757	4.20827E-04	1186.51	1178.76	1.38619E-03
22	18.348	2.82050E-04	1768.14	1840.31	1.00083E-03
23	21.3816	3.28683E-04	1442.8	1541.45	1.29748E-03
24	20.3947	3.13513E-04	1326.1	1408.98	1.19767E-03
25	29.2032	4.48920E-04	1030.57	1001.94	1.74938E-03
26	14.3275	2.20246E-04	2226.54	2147.02	7.65179E-04
27	6.25	9.60766E-05	4098.86	4194.19	4.07541E-04
28	9.64912	1.48329E-04	3164.03	3468.27	6.57056E-04
29	3.50877	5.39378E-05	7214	9017.5	2.57832E-04
30	4.56871	7.02315E-05	3920.65	5465.15	3.52093E-04
31	3.72807	5.73089E-05	4624.36	5009.72	3.52093E-04
32	3.50877	5.39378E-05	6011.67	7514.58	3.52093E-04
33	3.50877	5.39378E-05	5152.86	4624.36	2.82784E-04
		********AVERAGE********			
	NO.	NO./AREA	MFPV	MFPH	L/A
	23.414	3.59926E-04	1297.76	1324.33	1.32360E-03
SD	26.3264	4.04696E-04			1.39068E-03
SE	4.58284	7.04486E-05			2.42086E-04
34	96.4181	1.48216E-03	327.909	333.364	5.18159E-03
35	47.4415	7.29284E-04	648.741	626.215	2.63100E-03
36	51.8275	7.96706E-04	565.36	589.379	3.14943E-03
37	53.655	8.24798E-04	533.58	561.838	3.23260E-03
38	53.0336	8.15247E-04	445.309	568.927	3.32964E-03
39	19.9927	3.07333E-04	1528.39	1490.5	1.10064E-03
40	19.3348	2.97220E-04	1596.02	1654.59	1.12559E-03

41	12.6097	1.93839E-04	2470.55	2817.97	7.81813E-04
42	22.5877	3.47224E-04	1270.07	1345.9	1.35570E-03
43	17.617	2.70813E-04	1554.74	1541.45	1.11173E-03
44	8.40643	1.29226E-04	4098.86	3402.83	4.82395E-04
45	8.36988	1.28664E-04	3402.83	3920.65	4.93485E-04
46	4.82456	7.41644E-05	5635.94	5465.15	2.88328E-04
47	6.25	9.60766E-05	3837.23	3005.83	4.99030E-04
48	3.80117	5.84326E-05	5465.15	8197.73	3.54866E-04
49	2.37573	3.65204E-05	9017.5	10608.8	2.16246E-04
50	2.88743	4.43863E-05	7514.58	9492.1	2.05157E-04

********AVERAGE********

	NO.	NO./AREA	MFPV	MFPH	L/A
	24.0819	3.70193E-04	1236.8	1276.9	1.38436E-03
SD	26.0289	4.00123E-04			1.40161E-03
SE	3.68104	5.65859E-05			1.98217E-04

*

ORIGINAL PAGE IS
OF POOR QUALITY

```
 TT:=DX1:HEMA11.DAT
DEFECTS IN SILICON(VERSION 3-8/1/79)

JPL/HEM/4B-20/A-11   DISLOCSTION DENSITY

OPERATOR IS JMS  MAGNIFICATION=X800
UNITS= MM  CALIBRATION FACTOR (UNITS/PP)= 3.40700E-04
FRAME AREA= 500000  QTM OUTPUT WAS DIVIDED BY 1 AND CORRECTED
AVERAGE FEATURE AREA (PP)= 27.6
```

FLD	NO.	NO./AREA	MFPV	MFPH	L/A
1	73.0797	1259.16	.579422	.599824	2.70619
2	167.754	2890.4	.167833	.165228	10.0969
3	172.717	2975.92	.199707	.212937	8.00998
4	54.6377	941.408	.695306	.788657	2.24831
5	99.6377	1716.76	.343448	.338668	4.76079
6	222.391	3831.81	.137712	.13424	12.0869
7	98.9493	1704.9	.268268	.286303	5.98767
8	147.899	2548.3	.19924	.214008	8.00411
9	220.906	3806.21	.148647	.148518	11.0801
10	317.609	5472.4	.0986964	.0982411	16.8711
11	72.1015	1242.31	.437918	.448289	3.78926
12	59.3478	1022.56	.450661	.447113	3.68946
13	88.5507	1525.73	.329497	.328227	5.08659
14	157.572	2714.98	.185163	.204012	8.44438
15	413.696	7127.98	.0827745	.0875385	18.9169
16	98.0797	1689.92	.330136	.33402	4.90167
17	72.6087	1251.05	.371133	.354896	4.49663
18	193.116	3327.39	.1938	.197851	8.20957
19	130.036	2240.53	.225928	.221521	7.48459
20	101.558	1749.85	.285343	.275202	6.00822
21	73.6957	1269.78	.335996	.332715	4.85765
22	120.616	2078.22	.22444	.215633	7.69886
23	23.7319	408.901	.925815	1.00799	1.86968
24	235.471	4057.17	.153468	.153884	10.6898
25	119.13	2052.42	.233356	.241974	6.87702

********AVERAGE********

	NO.	NO./AREA	MFPV	MFPH	L/A
	141.396	2436.25	.22113	.224653	7.39489
SD	87.0243	1499.43			4.10924
SE	17.4049	299.886			.821848
26	110.109	1897.18	.270827	.257716	6.22542
27	111.449	1920.27	.245108	.230203	6.93279
28	308.732	5319.46	.126372	.137379	12.1896
29	301.812	5200.22	.128566	.131646	12.4186
30	258.659	4456.71	.129053	.127794	12.6827
31	214.239	3691.34	.148259	.136389	11.6378
32	139.275	2399.72	.195132	.185163	8.76431
33	92.5725	1595.03	.275202	.285822	5.92016
34	271.413	4676.45	.108711	.105089	15.2627
35	175.109	3017.13	.139403	.138609	11.7523
36	513.08	8840.37	.0711273	.0724277	22.8236
37	196.522	3386.07	.143998	.145598	11.1711
38	138.478	2385.98	.184761	.181416	9.09892
39	117.754	2028.9	.235942	.219241	7.39947
40	143.007	2464.02	.180839	.177079	9.15762
41	178.478	3075.18	.155855	.148518	10.6898
42	294.094	5067.25	.0978461	.0971763	16.8154
43	377.174	6498.71	.092481	.0931893	17.5844
44	90.1812	1553.82	.310858	.304741	5.42706
45	51.5942	888.969	.449472	.416504	3.93895

46	69.6015	1199.23	.371133	.362447	4.57881
47	178.333	3072.69	.153745	.152917	10.7162
48	291.63	5024.8	.113718	.107953	14.8723
49	169.964	2928.48	.144732	.149692	11.0332
50	150	2584.5	.179505	.176163	9.00206

********AVERAGE********

	NO.	NO./AREA	MFPV	MFPH	L/A
	169.563	2921.57	.181362	.181212	9.05935
SD	100.744	1735.82			4.54443
SE	14.2473	245.482			.642679

*

ORIGINAL PAGE IS
OF POOR QUALITY